Functional Characterization of a Non-AUUUA AU-Rich Element from the c-*jun* Proto-Oncogene mRNA: Evidence for a Novel Class of AU-Rich Elements

SHEILA S.-Y. PENG, CHYI-YING A. CHEN, AND ANN-BIN SHYU*

*Department of Biochemistry and Molecular Biology, The University of Texas Houston
Health Science Center, Medical School, Houston, Texas 77030*

AU-rich RNA-destabilizing elements (AREs) found in the 3′ untranslated regions of many labile mRNAs encoding proto-oncoproteins and cytokines generally contain (i) one or more copies of the AUUUA pentanucleotide and (ii) a high content of uridylate and sometimes also adenylate residues. Recently, we have identified a potent ARE from the 3′ untranslated region of c-*jun* proto-oncogene mRNA that does not contain the AUUUA motif. In an attempt to further our understanding of the general principles underlying mechanisms by which AREs direct rapid and selective mRNA degradation, in this study we have characterized the functionally important structural features and properties of this non-AUUUA ARE. Like AUUUA-containing AREs, this non-AUUUA ARE directs rapid shortening of the poly(A) tail as a necessary first step for mRNA degradation. It can be further dissected into three structurally and functionally distinct regions, designated domains I, II, and III. None of the three domains alone is able to significantly destabilize the stable β-globin mRNA. The two unlinked domains, I and III, together are necessary and sufficient for specifying the full destabilizing function of this non-AUUUA ARE. Domain II appears functionally dispensable but can partially substitute for domain I. Domain swaps made between the c-*jun* non-AUUUA and the c-*fos* AUUUA-containing AREs reveal that the two AREs, while sharing no sequence homology, appear to contain sequence domains that are structurally distinct but functionally overlapping and exchangeable. These data support the idea that the ultimate destabilizing function of an individual ARE is determined by its own unique combination of structurally distinct and functionally interdependent domains. Our polysome profile studies show that the destabilizing function of the c-*jun* non-AUUUA ARE does not require any active transit by ribosomes of the mRNA bearing it, further corroborating that the destabilizing function of AREs is not tightly coupled to ongoing translation by ribosomes. Moreover, unlike AUUUA-containing AREs, the c-*jun* ARE is insensitive to blockage of its effects by addition of transcription inhibitors. Thus, our data provide further evidence for the existence of a novel class of ARE with unique properties.

AU-rich RNA-destabilizing elements (AREs) are a group of loosely defined AU-rich instability determinants with sizes ranging from 50 to 150 nucleotides (nt) and are typically found in the 3′ untranslated region (UTR) of many highly labile mammalian mRNAs (3, 16). They represent the most common RNA stability determinant among those characterized in mammalian cells (for a recent review, see reference 14). Their presence in a wide variety of mRNAs including those encoding proto-oncoproteins, nuclear transcription factors, and cytokines suggests a critical role of the ARE in the regulation of gene expression during cell growth and differentiation of many cell types including those involved in the immune response (for a recent review, see reference 6). As different AREs vary considerably in their size and sequence content, important questions remain concerning what the functionally critical structure and sequence features are. For example, does a minimal core consensus sequence exist among different AREs that is necessary for their destabilizing function? Do all AREs belong to one class and target mRNA degradation through a common pathway, or can they be divided into different classes that may utilize distinct decay pathways?

Several important observations have recently been reported to address these issues. First, when present within a functional ARE, the AUUUA motifs have a destabilizing role (2, 4, 19).

A triple-point mutation that knocked out the three AUUUA motifs in the c-*fos* ARE resulted in a drastic retardation effect of the RNA destabilizing function (4). Moreover, in the case of interleukin-3 (IL-3) ARE, six AUUUA motifs are found in two clusters. Both clusters are required for a synergistic effect on RNA destabilization (19). Second, the mere presence of an AUUUA motif(s), even in an AU-rich region, does not guarantee a destabilizing function of an ARE (7, 13, 21). For example, we have shown that some AU-rich sequences (ARSs) from the labile early-response gene mRNAs, such as c-*jun*, *junB*, *krox20*, and *zif268*, possess the two general features of the ARE yet cannot confer instability on stable β-globin mRNA (7). Third, a general high content of uridylate residues within the ARE is required for its full destabilizing function. Our previous analysis of the c-*fos* ARE (4) has suggested that the 69-nt c-*fos* ARE contains two structurally distinct and functionally interdependent domains. Domain I has three copies of the AUUUA motif and confers a potent destabilizing ability by itself when tested in β-globin chimeric constructs. Domain II is a 20-nt U stretch that is interrupted by only three adenylate residues and has no destabilizing function (Fig. 1). In the absence of domain II, reduction of the U richness of domain I by replacement with G or C dramatically impairs its RNA-destabilizing function. However, this destabilization-retarding effect can be rescued by fusing it with the U-rich domain II immediately downstream from these domain I mutants, suggesting that domain II can complement the loss of U richness

* Corresponding author. Phone: (713) 792-5398. Fax: (713) 794-4150.

c-*jun* ARE

FIG. 1. RNA sequence of the c-*jun* and c-*fos* AREs. The 152-nt c-*jun* ARE sequence is shown on the top with GUUUG pentanucleotides underlined and domains I, II, and III bracketed. The polyadenylation signal (AAUAAA) within the c-*jun* ARE is indicated by bold characters and was changed to a *Bam*HI restriction site to create ARE*. The boundaries of various deletions shown in Fig. 3 and 4 are indicated by solid triangles. Asterisks mark the four nucleotides that were mutated from U to A in the ARE$^{c\text{-}jun}$ mutants 3′Δ1M4 and 5′Δ3M4 (Fig. 4). The italic, lowercase characters represent resultant nucleotides from the point mutations. The 69-nt human c-*fos* ARE sequence is shown on the bottom with AUUUA motifs underlined and domains I and II bracketed.

in domain I (4). Furthermore, several nonfunctional ARSs can be converted to potent destabilizing elements by placing the c-*fos* U-rich domain II immediately downstream of them (7). These examples illustrate the importance of U richness as an indispensable feature of functional AREs. Together, these observations indicate that the AUUUA motif and U richness are two critical sequence features among others, but they cannot fully account for the destabilizing function of an ARE. A functional ARE may involve higher-order organization of several structural features into functionally distinct domains.

The realization that the mere presence of AUUUA motifs is not always sufficient to ensure a destabilizing function of an ARS has invoked studies to search for other sequence motifs whose presence might guarantee the destabilizing ability of a newly identified ARS. By use of a series of synthetic AU-rich sequences, a nonamer with an AUUUA core, UUAUUUA(U/A)(U/A), was recently suggested to be a better indicator than the AUUUA motif in predicting the potential destabilizing function of an ARS (13, 21). It appears that functional AREs from cytokine transcripts, such as those encoding granulocyte-macrophage colony-stimulating factor (GM-CSF), beta interferon, and IL-3, have at least two overlapping copies of this nonamer within a highly U-rich region (6). However, several lines of evidence show that this nonamer represents neither the key sequence motif nor the minimal consensus core present in all of the different AREs described to date. First, insertion of a single copy of the nonamer into the 3′ UTRs of reporter mRNAs had only a modest effect on the stability of the reporter mRNAs, with a 4-h time lag before the decay of RNA body commenced (13, 21). Second, many known functional AREs from early-response gene mRNAs, such as c-*myc*, *junB*, c-*jun*, and *nur77* AREs, do not contain this nonamer (7). Finally, although in the c-*fos* ARE the two overlapping AUUUA motifs give rise to a single copy of the nonamer (Fig. 1), several single point mutations that knocked out this nonamer have little effect on the RNA-destabilizing function of the c-*fos* ARE (4). On the basis of these observations, it is likely that the nonamer may be one of the critical sequence features for only some AREs (see below).

On the basis of the data summarized above, we have previously proposed the existence of at least three classes of ARE (6, 7). They can be divided into two groups: AUUUA-containing and non-AUUUA AREs. The AUUUA-containing AREs may be further divided into two distinct classes. Class I consists of AREs from some early-response gene mRNAs that encode nuclear transcription factors. They contain a few copies of scattered AUUUA motifs coupled with nearby U-rich sequences. Class II includes those from some cytokine mRNAs and tends to have multiple reiterations of AUUU tetranucleotides which contribute to a general high uridylate content. Since multiple reiterations of the AUUU tetranucleotide concomitantly give rise to an RNA sequence having at least two overlapping nonamers, the nonamer may be one of the key sequence motifs that define class II AUUUA-containing AREs. In addition, it should be noted that neither the AUUUA motif nor the nonamer need be an integral part of a functional ARE.

In an effort to further define the critical structural features that are necessary and sufficient to specify the destabilizing function of AREs and to search for more evidence to support the existence of distinct classes of ARE proposed above, in this study we have characterized a non-AUUUA ARE from c-*jun* proto-oncogene mRNA. Our results provide evidence that the c-*jun* non-AUUUA ARE represents a novel class of ARE. More importantly, they support the idea that AREs can be functionally overlapping and possess structurally distinct sequence motifs or domains, such as AUUUA motifs, UUAUUUA(U/A)(U/A) nonamers, U stretches, and U-rich domains. We propose that it is the combination of these sequence and structural features within an ARE that determines the ultimate destabilizing function of that particular ARE.

MATERIALS AND METHODS

Cell culture and DNA transfection. Culturing, transient transfection, and serum stimulation of mouse NIH 3T3 cells were performed as described previously (18). Actinomycin D and 5,6-dichloro-1-β-D-ribofuranosylbenzimidazole (DRB) were purchased from Sigma Chemical Co.

Plasmid constructions. Construction of the plasmids pSVα1/GAPDH and pBBB+ARE$^{c\text{-}jun}$ has been described previously (4, 7). To construct pBBB+

ARE^{c-jun*}, sequences encoding the polyadenylation signal (AAUAAA) within the c-*jun* ARE were changed to a *Bam*HI site (Fig. 1) by recombinant PCR mutagenesis (9) with plasmid pBBB+ARE^{c-jun} as the template.

To construct all the deletion mutants as shown in Fig. 3 and 4, various regions of c-*jun* ARE were amplified by standard PCR techniques (9). Plasmid pBBB+ARE^{c-jun*} was used as the template for construction of the mutants shown in Fig. 3. One of the resultant deletion mutant (3′Δ1), in which the last 6 nt from the c-*jun* ARE* was deleted, was used as the template for construction of the deletion mutants shown in Fig. 4. Sequences of the amplified fragments are shown in Fig. 1. All the PCR-amplified fragments (with the exception of those for 5′Δ1 and d1) are flanked either by *Bgl*II sites at both ends or by a *Bam*HI site at one end and a *Bgl*II site at the other end. After *Bgl*II or *Bam*HI-*Bgl*II digestion, the fragments were introduced into the unique *Bgl*II site of plasmid pBBB (18), which is immediately downstream of the translation termination codon. The PCR-amplified fragments for 5′Δ1 and d1 were blunt ended with Klenow enzyme and inserted into the unique *Bgl*II site (blunt ended with Klenow enzyme) of pBBB.

To construct pBBB+ARE(fI/jI) and pBBB+ARE(fI/jI+3), the c-*jun* ARE domain I and domain I plus subregion 3 were amplified by standard PCR techniques (9) with pBBB+ARE^{c-jun*} as the template. The PCR-amplified fragment for c-*jun* ARE domain I is flanked by *Bgl*II sites at both ends, and that for c-*jun* ARE domain I plus subregion 3 is flanked by a *Bgl*II site at the 5′ end and a *Bam*HI site at the 3′ end. After *Bgl*II or *Bam*HI-*Bgl*II digestion, the fragments were introduced into the unique *Bgl*II site of plasmid pBBB+AREI^{c-fos} (4), which is immediately downstream from the c-*fos* ARE domain I. To construct pBBB+ARE(fII/jIII) and pBBB+ARE(fII/jIII+4), the c-*jun* ARE domain III and domain III plus subregion 4 were amplified by standard PCR techniques with pBBB+ARE^{c-jun*} as templates. Both PCR-amplified fragments are flanked by a *Bam*HI site at their 5′ ends and a *Bgl*II site at their 3′ ends. After *Bam*HI and *Bgl*II digestion, the fragments were introduced into the unique *Bgl*II site of plasmid pBBB+AREII^{c-fos} (4), which is immediately downstream from the c-*fos* ARE domain II.

The plasmid BBB+ARE^{c-jun}-hp was constructed by replacing a 379-bp *Bss*HII-*Acc*I fragment of pBBB+ARE^{c-jun*} derivative designated 3′Δ1 (see Fig. 3), which spans sequences encoding the last 85 nt of the c-*fos* promoter region, the first 160 nt of the β-globin mRNA 5′ UTR, and part of the β-globin coding region, with a 430-bp *Bss*HII-*Acc*I fragment from pBBB+ARE^{c-fos}-hp (5), which encodes the same region as described above and has a desired hairpin (12) inserted 20 bp downstream of the transcription initiation site of the β-globin gene (5).

Analysis of mRNA decay and deadenylation. Total cytoplasmic RNA was isolated at various times after serum stimulation of transiently transfected NIH 3T3 cells, and the mRNA decay and deadenylation were analyzed by Northern (RNA) blot analysis as described previously (17, 18). To analyze the mRNA decay, α-glyceraldehyde-3-phosphate dehydrogenase (α-GAPDH) (7) was used in transient-transfection experiments as an internal control. Electrophoresis was done on 1.4% formaldehyde agarose gels. A 123-nt single-stranded DNA ladder (Bethesda Research Laboratories [BRL]) was included to provide a molecular size standard. Gene-specific DNA probes were prepared by the method of random oligonucleotide priming. Labeled probes were produced by inclusion of [α-^{32}P]dCTP (>6,000 Ci/mmol; Amersham). RNase H treatment of cytoplasmic mRNA was carried out as described previously (17). Decay of mRNA was quantitated directly by scanning blots on a Betascope 603 Blot Analyzer (Betagen). To determine the half-life for each BBB+ARE gene construct, time course experiments were carried out at least twice. A representative value for the half-life from one of the duplicate experiments was reported for each BBB+ARE mRNA.

Polysome profile analysis. Analyses of polysome profile by sucrose gradient fractionation and subsequent analyses of specific distribution of tested mRNAs as well as the control α-GAPDH mRNA in the fractions were performed as described previously (5).

RESULTS

Differential polyadenylation results in two mRNAs carrying different extents of the c-*jun* non-AUUUA ARE that exhibit different turnover rates. Previously, using an RNase protection assay, we identified a 152-nt non-AUUUA ARE from the 3′ UTR of c-*jun* mRNA (Fig. 1) that is able to destabilize the normally stable β-globin mRNA (7). To further study the decay kinetics of this novel ARE, Northern blotting was used to determine not only the half-life of the β-globin mRNA bearing the ARE but also the deadenylation pattern of the mRNA. The β-globin gene containing the c-*jun* ARE in its 3′ UTR (BBB+ARE^{c-jun}), whose transient expression was driven by the c-*fos* promoter, was introduced into NIH 3T3 cells by transient cotransfection with a control gene. The control mRNA, designated α-GAPDH, was constitutively expressed as an in-
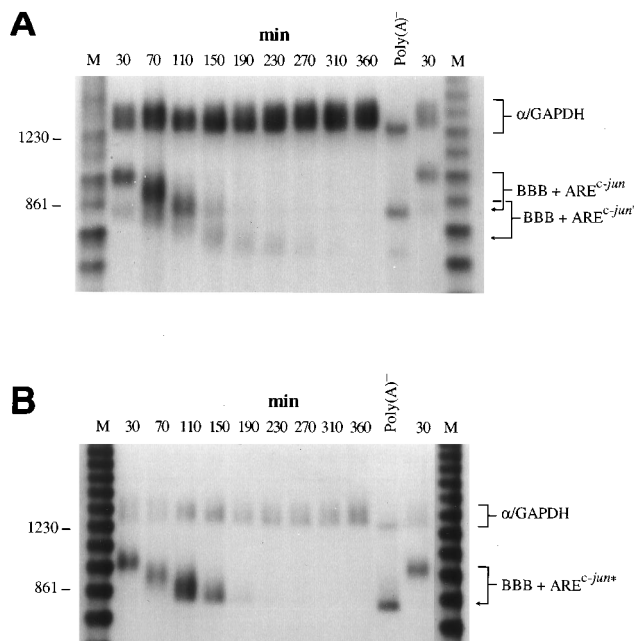

FIG. 2. Differential polyadenylation results in two mRNAs carrying different extents of the c-*jun* non-AUUUA ARE that exhibit different turnover rates. NIH 3T3 cells were transiently cotransfected with the control plasmid pSVα1/GAPDH and either the plasmid carrying the 152-nt wild-type c-*jun* ARE (A) or the c-*jun* ARE* (B). Total cytoplasmic mRNA was isolated at various time intervals after serum stimulation. α-GAPDH mRNA was expressed constitutively and served as an internal standard for the experiments. The mRNA decay and deadenylation was analyzed by Northern blot analysis. The times given on the top correspond to minutes after serum stimulation. At 30 min after serum induction, BBB+ARE mRNAs still retained a full-length poly(A) tail (~200 nt). Poly(A)$^-$ RNA was prepared in vitro by treating RNA samples from the 30-min time points with oligo(dT) and RNase H. The 123-bp DNA ladder from BRL was used as a molecular size standard. Positions corresponding to 861 and 1,230 nt are indicated.

ternal standard to correct variations in transfection efficiency and sample handling (7). Transcription of the BBB+ARE^{c-jun} gene and its derivatives was then transiently induced by stimulation of the c-*fos* promoter with 20% calf serum. Total cytoplasmic mRNA was isolated at time intervals and analyzed by Northern blotting.

As shown in Fig. 2A, two mRNAs with a size difference of approximately 170 nt were detected. The longer mRNA (BBB+ARE^{c-jun}) has a 37-min half-life, and the shorter one (BBB+ARE$^{c-jun'}$) has a 70 min half-life. Interestingly, both mRNAs underwent decay with a biphasic pattern that is characteristic of the c-*fos* ARE-mediated mRNA degradation, i.e., rapid deadenylation followed by decay of the RNA body (4). Since the c-*jun* ARE contains an AAUAAA polyadenylation signal ~170 nt upstream from the polyadenylation signal present in the 3′ UTR of the BBB-ARE^{c-jun} mRNA (Fig. 1), it is possible that the longer mRNA was derived from 3′-end processing with the β-globin polyadenylation signal whereas the shorter one resulted from utilizing the AAUAAA signal within the c-*jun* ARE. To examine this possibility, the polyadenylation signal within the c-*jun* ARE was inactivated by site-directed mutagenesis and, concomitantly, a *Bam*HI site was created (Fig. 1). This mutant ARE was designated ARE*. Northern blot analysis (Fig. 2B) showed that the mutation abolished the formation of the shorter mRNA but not the longer one, demonstrating that the two mRNAs result from differential polyadenylation. Since the AAUAAA mutation within the c-*jun*
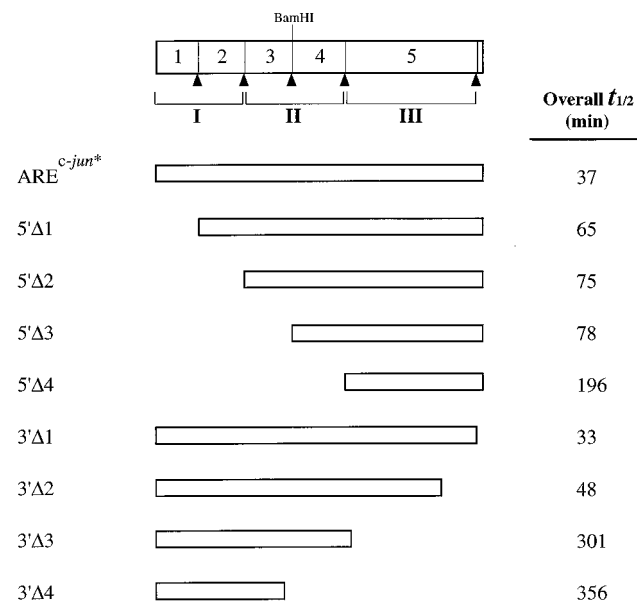
FIG. 3. End mapping of the c-*jun* ARE by deletion analysis. The sequence of the c-*jun* ARE is shown in Fig. 1. The solid triangles indicate the endpoints of each deletion. Open rectangles represent those ARE regions retained in the deletion constructs. Total cytoplasmic mRNA was isolated at various time intervals after serum stimulation and analyzed by Northern blot analyses as described in the legend to Fig. 2. Quantitation of data was performed by scanning the radioactive blots with a Betascope blot analyzer (the Betagen). The overall half-life ($t_{1/2}$) measured mRNA decay starting at 70 min postinduction, when transcription from the c-*fos* promoter returned to preinduction levels.

ARE has no adverse effect on the destabilizing function of the c-*jun* ARE and eliminates the generation of the shorter mRNA (Fig. 2B), it was used for subsequent experiments.

The c-*jun* ARE consists of three functionally distinct domains. As an initial step to characterize the structural features of the c-*jun* ARE that specify its RNA-destabilizing function, two sets of nested deletions, one set from the 5′ end and the other from the 3′ end of the 152-nt ARE*, were created to map its minimal boundaries. The resulting truncated derivatives of ARE* were tested for their abilities to destabilize the stable β-globin mRNA (Fig. 3) (4). Deletion of the first 21 nt from the 5′ end of the ARE* (Fig. 3, 5′Δ1) retarded its destabilizing function by ~1.8-fold. The β-globin mRNA carrying this truncated ARE* decayed with a half-life of ~65 min, indicating that the 5′ end of the functional c-*jun* ARE is located in this 21-nt segment. Further deletions up to the *Bam*HI site of the ARE* (Fig. 3, 5′Δ2 and 5′Δ3) resulted in little change of the RNA half-life, suggesting that some internal regions are functionally dispensable. When the endpoint of deletion extended 28 nt downstream from the *Bam*HI site (Fig. 3, 5′Δ4), the half-life of the mRNA was significantly increased to ~200 min.

When the effects of various 3′ deletions of the ARE* were determined (Fig. 3), the results showed that the last 6 nt can be deleted (3′Δ1) without any effect and that deletion of the last 20 nt (3′Δ2) slightly reduced the destabilizing function of the ARE* by ~1.5-fold. Deletion of the GU-rich sequence (3′Δ3) resulted in an eightfold retardation of the ARE* destabilizing function. Further deletion to the *Bam*HI site (3′Δ4) had a 10-fold stabilization effect. Taken together, the mapping data showed that at least 6 nt from the 3′ end of the ARE* can be deleted without significantly affecting its RNA destabilizing function. Thus, the resultant 146-nt ARE (3′Δ1) was used for all subsequent functional characterizations of the c-*jun* ARE.

Since we have shown that the c-*fos* ARE can be dissected into two different domains, we were interested in learning whether the c-*jun* ARE may also be composed of distinct domains. To identify and characterize the functional domains that may constitute the c-*jun* ARE, the ARE was divided into five subregions (Fig. 3 and 4) with endpoints defined by deletion analysis (Fig. 3). As described above, our results from the 5′-end mapping experiments (Fig. 3) have suggested that some internal regions are functionally dispensable. We then further determined which of the subregions are functionally dispensable. A series of deletions were created to precisely remove each of the five subregions from the ARE (Fig. 4). Time course experiments were carried out to analyze the destabilizing function of these mutant AREs. The results showed that subregion 3 or 4 can be deleted without affecting the destabilizing ability of the c-*jun* ARE whereas deletion of subregion 2 has a modest stabilization effect. The greatly increased half-lives of 3′Δ3 (Fig. 3 and 4) indicate that deletion of subregion 5 essentially abolished the destabilizing function. These results indicate that the GU-rich subregion 5 may serve as an essential backbone for the c-*jun* ARE. Further internal deletion to remove both subregions 3 and 4 (Fig. 4, ΔII) had a very mild effect on the destabilizing function of the c-*jun* ARE, demonstrating that these two subregions together are functionally dispensable and
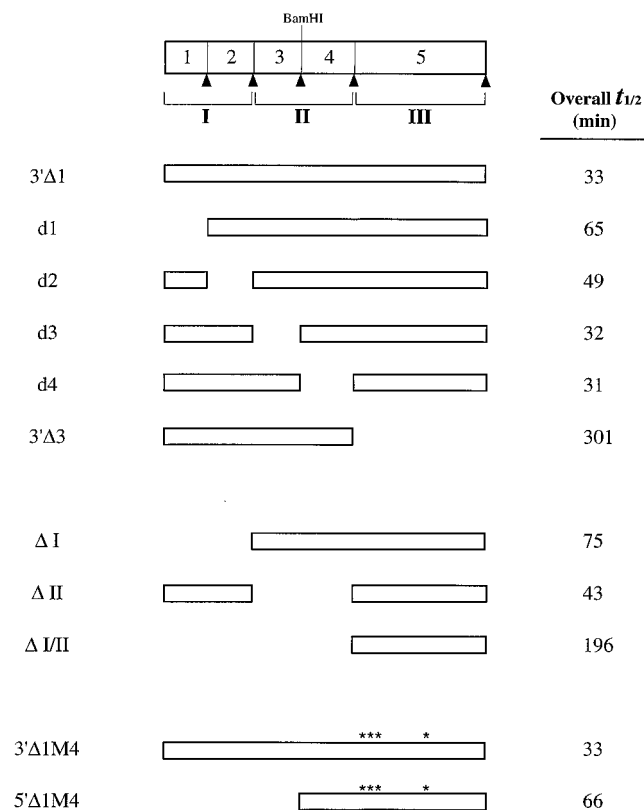

FIG. 4. Characterization of the functional domains of the c-*jun* ARE. Sequence of the c-*jun* ARE is shown in Fig. 1. The solid triangles indicate the endpoints of each deletion. Open rectangles represent those ARE regions retained in the deletion constructs. Asterisks mark the four nucleotides that were mutated from U to A in the ARE$^{c\text{-}jun}$ mutants 3′Δ1M4 and 5′Δ3M4 (Fig. 1). Total cytoplasmic mRNA was isolated at various time intervals after serum stimulation and analyzed by Northern blot analyses as described in the legend to Fig. 2. Quantitation of data was performed by scanning the radioactive blots with a Betascope blot analyzer (the Betagen). The overall half-life ($t_{1/2}$) measured mRNA decay starting at 70 min postinduction, when transcription from the c-*fos* promoter returned to preinduction levels.
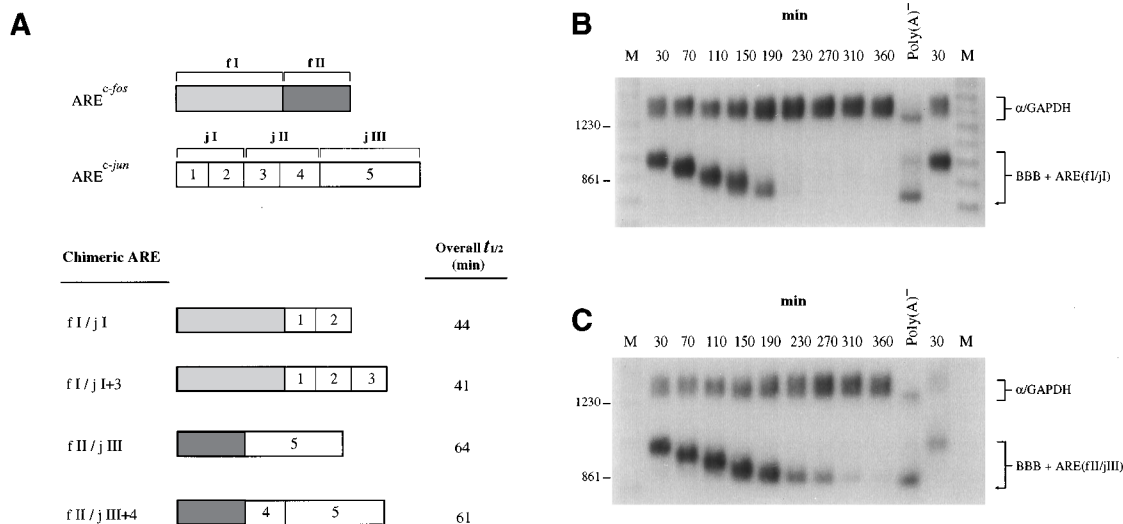
FIG. 5. Functionally overlapping domains exist between the c-*fos* and c-*jun* AREs. (A) Schematic diagram of chimeric AREs and summary of the decay rates for the β-globin mRNA carrying these hybrid AREs. fI, c-*fos* domain I; fII, c-*fos* domain II; jI, c-*jun* domain I; jII, c-*jun* domain II; jIII, c-*jun* domain III. (B) RNA blot showing decay of the β-globin mRNA carrying the chimeric ARE(fI/jI). (C) Decay of the β-globin mRNA carrying the chimeric ARE(fII/jIII). Total cytoplasmic mRNA was isolated at various time intervals after serum stimulation and analyzed by Northern blot analyses as described in the legend to Fig. 2. Quantitation of data was performed by scanning the radioactive blots with a Betascope blot analyzer (the Betagen). The overall half-life ($t_{1/2}$) measured mRNA decay starting at 70 min postinduction when transcription from the c-*fos* promoter returned to preinduction levels. Poly(A)$^-$ RNA was prepared in vitro by treating RNA samples from the 30-min time points with oligo(dT) and RNase H. The 123-bp DNA ladder from BRL was used as a molecular size standard. Positions corresponding to 861 and 1,230 nt are indicated. The overall half-lives are 60 ± 26 min for BBB+fI, 196 ± 45 min for BBB+jIII, 35 ± 8 min for BBB+ARE$^{c\text{-}fos}$, and 37 ± 9 min for BBB+ARE$^{c\text{-}jun}$ mRNAs.

are not necessary for the destabilizing function of the ARE. Deletion of both subregions 1 and 2 (Fig. 4, ΔI) caused a two-fold retardation effect on the destabilizing function of the c-*jun* ARE. However, further deletion covering subregions 1 to 4 (Fig. 4, ΔI/II) has a severe decay-impeding effect (~5.3-fold). This result indicates that even though subregions 3 and 4 together are dispensable, when subregions 1 and 2 are deleted, subregions 3 and 4 become necessary and are able to cooperate with subregion 5 to exert a fairly potent destabilizing effect. On the basis of these deletion analyses, we conclude that the c-*jun* ARE can be divided into at least three functionally distinct but interdependent domains (Fig. 4): domain I (subregions 1 and 2), domain II (subregions 3 and 4), and domain III (subregion 5). The two unlinked domains, I and III, together are necessary and sufficient for directing rapid mRNA decay by the c-*jun* ARE, whereas domain II appears fully dispensable but can partially substitute for domain I.

Although domain III is not sufficient to confer a drastic destabilizing effect on the stable β-globin mRNA, it is the most critical domain of the c-*jun* ARE, because its deletion resulted in a nearly complete loss of the RNA-destabilizing function of the ARE (Fig. 3 and 4). One interesting sequence feature in this domain is the presence of four copies of a GUUUG motif. Since the GUUUG and AUUUA motifs represent a stretch of triple uridylate residues flanked by purine residues, we were interested in learning whether the two motifs may be functionally equivalent. Four single-point mutations were simultaneously introduced into domain III of the 3'Δ1 ARE and the 5'Δ3 ARS to change each of the four copies of GUUUG motifs within domain III to GUAUG or GAUUG pentanucleotides (Fig. 1 and 4, 3'Δ1M4 and 5'Δ3M4). The destabilizing function of these ARE derivatives was not affected by these four point mutations (Fig. 4). We therefore conclude that the GUUUG pentamer is not a critical sequence motif for the function of the c-*jun* ARE.

Functionally overlapping and exchangeable domains between the c-*fos* and c-*jun* AREs. The observation that the c-*jun*

ARE can be divided into functionally distinct but interdependent domains is also true for the c-*fos* ARE. The destabilizing function of the c-*fos* ARE is determined by the interaction of two domains (4). Domain I is an essential backbone whose destabilizing function can be enhanced by domain II, located immediately downstream from it. While domain II by itself has no destabilizing function, it can buffer against the decay-impeding effect caused by mutations that are introduced into domain I. Moreover, domain II can function even when placed upstream of domain I (4). Therefore, it appears that c-*fos* domain I and c-*jun* domain III are functionally similar whereas c-*jun* domains I and II share similar properties with c-*fos* domain II. To identify domains of the two AREs that may be functionally analogous and therefore exchangeable, several chimeric AREs were created by making domain swaps between the two AREs (Fig. 5A). Remarkably, while c-*jun* domain I and c-*fos* domain II share no sequence homology and contain different extents of uridylate residues, they are functionally overlapping. As shown in Fig. 5B, the fI/jI hybrid ARE not only directs β-globin mRNA decay with a half-life similar to that of the wild-type c-*fos* ARE but also directs mRNA decay with biphasic kinetics, demonstrating that the c-*jun* domain I can substitute the c-*fos* domain II for its function. Similarly, the fII/jIII hybrid ARE (Fig. 5C) can also reduce the half-life of β-globin mRNA from greater than 10 h to 64 min, albeit to a lesser extent than the c-*jun* ΔII, which contains c-*jun* ARE domains I and III and has a half-life of 43 min. These results show that functionally the c-*fos* domain II is similar to the c-*jun* domain I. Further inclusion of subregion 4 from the c-*jun* ARE to the fII/jIII construct (Fig. 5A, fII/jIII+4) did not lead to any significant increase of the destabilizing function of the fII/jIII hybrid ARE. In addition, inclusion of subregion 3 from the c-*jun* ARE to the fI/jI hybrid ARE (Fig. 5A, fI/jI+3) did not invoke further enhancement of the destabilizing effect. These results substantiate the dispensable nature of subregions 3 and 4 within the c-*jun* ARE.

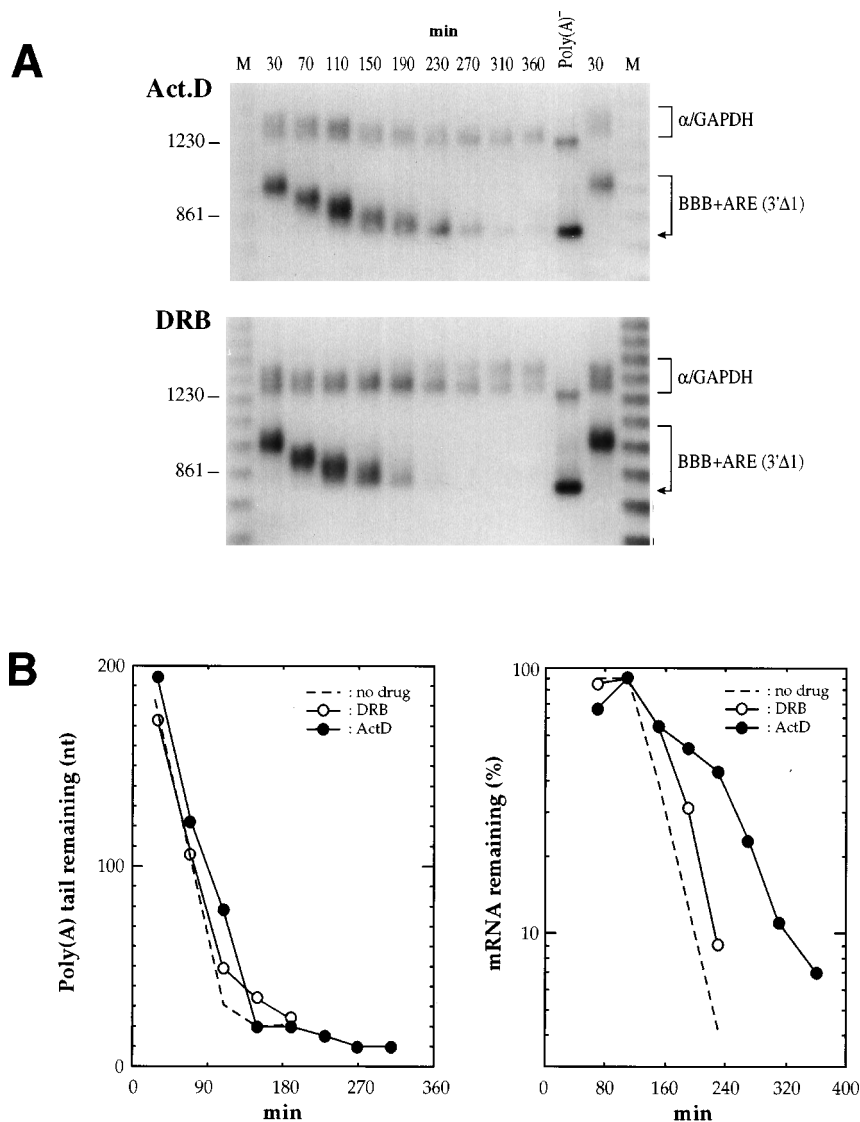Taken together, our data show that the c-*jun* ARE consists

FIG. 6. The destabilizing function of the c-*jun* ARE is not affected by the transcription inhibitors actinomycin D and DRB. (A) Northern blot showing that the c-*jun* ARE is able to destabilize the β-globin mRNA in the presence of actinomycin D (Act.D) (upper panel) or DRB (lower panel). Transient cotransfection of NIH 3T3 cells with the control plasmid pSVα1/GAPDH and pBBB+ARE$^{c\text{-}jun}$(3′Δ1) and subsequent analysis of mRNA decay were carried out as described in the legend to Fig. 2. The times given on the top correspond to minutes after serum stimulation. Actinomycin D (5 μg/ml) or DRB (20 μg/ml) was added to the culture medium 30 min after serum induction. Poly(A)$^−$ RNA was prepared in vitro by treating RNA samples from the 30-min time points with oligo(dT) and RNase H. The 123-bp DNA ladder from BRL was used as a molecular size standard. Positions corresponding to 861 and 1,230 nt are indicated. (B) The time courses of deadenylation (left) and the decay (right) of β-globin mRNA carrying the c-*jun* ARE (3′Δ1) as shown in panel A are plotted. Quantitation of data was performed by scanning the radioactive blots with a Betascope blot analyzer (Betagen).

of structurally different and functionally distinct domains and that functionally overlapping domains may exist between the AUUUA-containing c-*fos* ARE and the non-AUUUA c-*jun* ARE.

The non-AUUUA ARE from c-*jun* mRNA is functionally distinct from the AUUUA-containing AREs and can be uncoupled from translation. Previously, we have shown that the destabilizing function of the two classes of AUUUA-containing AREs can be fully abolished by actinomycin D and partially inactivated by DRB (5). In addition, their destabilizing function can be uncoupled from translation by ribosomes (5). To further characterize the novel non-AUUUA c-*jun* ARE, we carried out experiments to address how the c-*jun* ARE would respond to transcription inhibitors and to targeted inhibition of its translation by hairpin insertion.

First, the potential decay-impeding effect of transcription inhibitors was examined. At 30 min after serum induction of the expression of the β-globin mRNA carrying the c-*jun* ARE, either actinomycin D or DRB was added to the culture medium and mRNA decay was subsequently monitored by Northern blot analysis (Fig. 6). Consistent with our previous finding (5), the α-GAPDH mRNA exhibited slow decay after transcription was inhibited by actinomycin D. Remarkably, treatment of NIH 3T3 cells with actinomycin D only slightly retarded the c-*jun* ARE destabilizing function. The β-globin mRNA carrying the c-*jun* ARE underwent rapid decay, which is in contrast to a complete stabilization by actinomycin D of β-globin mRNA carrying either the c-*fos* ARE or the GM-CSF ARE (5). When decay kinetics were examined, actinomycin D did not alter the deadenylation kinetics and decay of the RNA

body following deadenylation was only slightly impaired. Moreover, DRB had no retardation effect on c-*jun* ARE-mediated mRNA degradation (Fig. 6). These results support the notion that this non-AUUUA ARE represents a novel class of ARE.

Second, to address whether this novel ARE requires translation to function as a destabilizing element, translation initiation of the β-globin mRNA carrying the c-*jun* ARE was blocked by inserting a stable hairpin ($\Delta G = -61$ kcal [ca. -255 kJ]/mol) in its 5′ UTR (5, 12). By examining polysome profiles, we previously showed that this approach successfully blocked translation initiation of the β-globin mRNAs carrying various AREs (5). As shown in Fig. 7, hairpin insertion had a rather modest stabilizing effect. It led to a 1.5-fold increase in the half-life for the β-globin mRNA bearing c-*jun* ARE, from 33 to 51 min. There is little change in the deadenylation step. This result demonstrated that in common with the AUUUA-containing AREs, decay directed by this non-AUUUA ARE can be uncoupled from ongoing translation by ribosomes.

DISCUSSION

In this study, we have used deletion analyses to demonstrate that the c-*jun* ARE consists of three individual domains, I, II, and III. Domain I contains a 20-nt alternating thymidylate and purine region and, alone, is not able to destabilize the stable β-globin mRNA. However, when it is fused with domain III, a destabilizing function similar to that of the intact c-*jun* ARE is produced. Domain II is the least AU-rich sequence among the three domains (58% A+U residues) and, alone, cannot confer instability. Although domain II appears functionally dispensable, since its deletion from the c-*jun* ARE has only a very mild (~1.3-fold) retardation effect on the RNA destabilizing function, it can partially substitute for domain I. Interestingly, there is no apparent sequence homology between domain I and domain II. Domain III may constitute the backbone of the c-*jun* ARE, since its deletion has the most dramatic retardation effect on the destabilizing function of the c-*jun* ARE. In addition, unlike domains I and II, domain III alone has some destabilizing capability. Through its interaction with the other two domains, the full destabilizing function of the c-*jun* ARE domain III may thus be specified. One interesting feature of domain III is that it is a GU-rich sequence with four copies of a GUUUG motif. Point mutations that change each of the four GUUUG motifs to GUAUG or GAUUG in the c-*jun* ARE do not result in any detectable change in the original destabilizing function. Therefore, unlike the functional role played by the AUUUA motifs in the AUUUA-containing AREs (6), the GUUUG pentanucleotide is apparently not a critical sequence feature. Since domain III is the only region among all known AREs that is rich in guanylate nucleotides, it will be interesting to determine whether these G residues possess a role in RNA destabilization.

It is worth noting that the half-lives of the short transcript in Fig. 2 (BBB+ARE^c-*jun*′; $t_{1/2} \approx 70$ min) and the domain III deletion in Fig. 3 (3′Δ3; $t_{1/2} \approx 301$ min) are different. The fundamental difference between these two mRNAs is that the BBB+ARE^c-*jun*′ mRNA resulted from utilizing the AAUAAA signal within the c-*jun* ARE and the 3′Δ3 mRNA was derived from 3′-end processing by using the β-globin polyadenylation signal. Although the two mRNAs carry similar extent of the c-*jun* ARE, their 3′ UTRs are different. The 3′ UTR of 3′Δ3 consists of the first 65% of the c-*jun* ARE followed by the β-globin 3′ UTR, and the ARE is located 90 nt upstream from the 3′ poly(A) tail. In contrast, the 3′ UTR of BBB+ARE^c-*jun*′ consists of only the first 65% of the c-*jun* ARE, and therefore,

the ARE is immediately upstream of the 3′ poly(A) tail. It is possible that their stability difference is due to the difference in their relative positions with respect to the poly(A) tail or that the presence of the β-globin 3′ UTR in the 3′Δ3 mRNA interfered with the residual ARE function, or both.

One of the intriguing observations in this study is that two structurally distinct domains, one from the c-*jun* ARE and the other from the c-*fos* ARE, can essentially substitute for each other's functional role in the original ARE. When a reciprocal exchange of c-*jun* and c-*fos* ARE domains was made, both new chimeric (fI/jI and fII/jIII) AREs exhibited destabilizing functions close to those of the two original AREs (Fig. 5). This observation corroborates the proposed existence of functionally overlapping domains in different AREs. It should be noted that there is a subtle functional distinction between c-*fos* domain II and c-*jun* domain I. The c-*jun* domain I appears able to enhance the destabilizing function of the c-*fos* domain I, so that the final destabilizing function of the hybrid ARE(fI/jI) (Fig. 5) parallels that of the wild-type c-*fos* ARE, whereas the c-*fos* domain II can only partially restore the destabilizing function of the c-*jun* domain III. Therefore, c-*fos* domain II and c-*jun* domain I are functionally overlapping but not equivalent.

Thus, from the dissection of the two AREs, we have identified a group of three sequence domains, c-*fos* domain II, c-*jun* domain I, and c-*jun* domain II, that share some similar properties. First, they all can boost the destabilizing function of c-*jun* domain III when fused upstream of it, albeit to different extents. Second, they all can be deleted from the cognate ARE without causing a severe retardation effect. Third, they cannot confer instability onto the stable β-globin mRNA by themselves. It is possible that these modular sequences or domains help facilitate their partner domains, such as c-*jun* domain III and c-*fos* domain I, to recruit cellular factors to form the decay machinery that mediates deadenylation and subsequent decay of the RNA body. It is worth noting that while c-*jun* domain I and c-*fos* domain II share no significant sequence homology, they can be recognized by a similar set of cytoplasmic factors but with different affinity (unpublished observation). This suggests that the decay-enhancing function of each individual domain is determined at least in part by the way it interacts with cognate *trans*-acting factors.

Previously, we proposed that there are three different classes of ARE (6, 7). In this study, we have provided further evidence to support the existence of distinct classes of ARE and have added several new criteria that help to refine the classification of AREs (Table 1). While all three classes of ARE direct rapid deadenylation as a critical first step in triggering subsequent decay of the transcribed portion of mRNA, there is an important difference in the deadenylation reaction that distinguishes the three classes. Class I AUUUA-containing AREs and non-AUUUA AREs both direct a synchronous shortening of poly(A) tails to 30 to 60 nt before decay of the mRNA body commences, which is likely to be a result of distributive enzymatic action (4, 5). In contrast, class II AUUUA-containing ARE mediates an asynchronous deadenylation, with the formation of fully deadenylated intermediates, consistent with the action of a processive ribonucleolytic digestion of poly(A) tails (5). Thus, these results also explain why apparent decay kinetics of the non-AUUUA ARE and the class I AUUUA-containing ARE differ from those of the class II AUUUA-containing ARE (5).

Recent studies by Hirsch et al. (10) concerning the RNA-destabilizing function of IL-3 ARE lend further support to our classification. They showed that rapid degradation of IL-3 mRNA in a cloned IL-3-dependent mast cell line, PB-3c, is
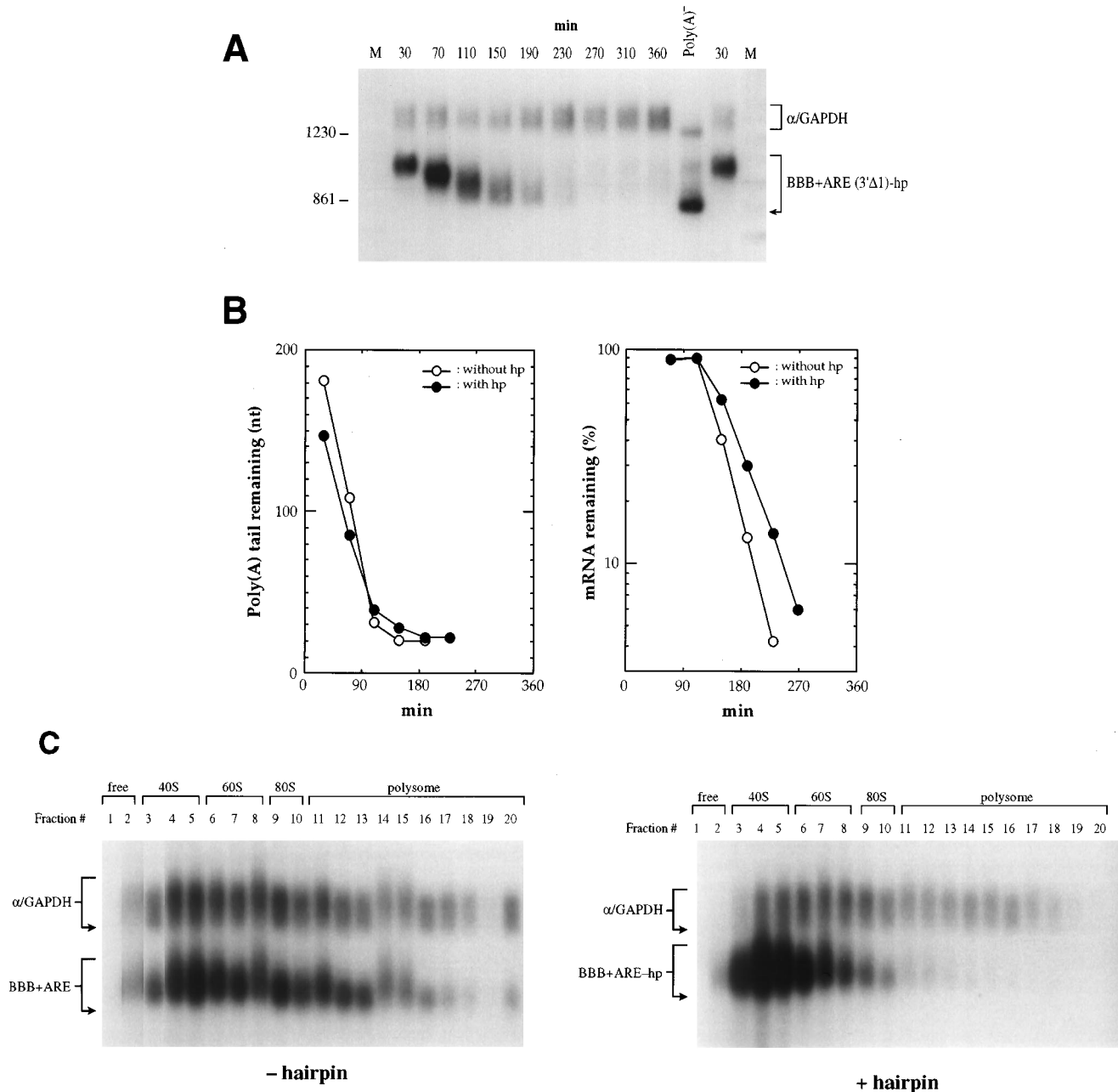
FIG. 7. The RNA-destabilizing function of the c-*jun* ARE can be uncoupled from ongoing translation by ribosomes in NIH 3T3 cells. (A) Northern blot showing the decay of pBBB+ARE$^{c\text{-}jun}$-hp mRNA. Transient cotransfection of NIH 3T3 cells with the control plasmid pSVα1/GAPDH and pBBB+ARE$^{c\text{-}jun}$-hp and subsequent analysis of mRNA decay were carried out as described in the legend to Fig. 2. The times given on the top correspond to minutes after serum stimulation. Poly(A)$^-$ RNA was prepared in vitro by treating RNA samples from the 30-min time points with oligo(dT) and RNase H. The 123-bp DNA ladder from BRL was used as a molecular size standard. Positions corresponding to 861 and 1,230 nt are indicated. (B) The time courses of deadenylation (left) and the decay (right) of β-globin mRNA carrying the c-*jun* ARE (3′Δ1) with or without hairpin insertion to block translation initiation are plotted. Quantitation of data was performed by scanning the radioactive blots with a Betascope blot analyzer (Betagen). (C) The distribution of BBB+ARE$^{c\text{-}jun}$ mRNA without the hairpin (left) or with the hairpin (right) and the internal control mRNA (α/GAPDH mRNA) in the polysome profile were identified by Northern blotting. Cells transiently cotransfected with the corresponding constructs were serum starved for 25 h and then serum induced for 30 min. Cytoplasmic lysates were prepared and fractionated through a continuous sucrose gradient (15 to 40%) to resolve the ribosome subunits and polysomes (for details, see reference 5). Polysome profiles were obtained by running RNA samples from each fraction onto a 1% agarose gel, which was subsequently stained with ethidium bromide (data not shown). Positions of the 40S, 60S, and 80S ribosomal subunits, as well as polysomes, are marked.

mediated by a 39-nt ARE in the 3′ UTR of IL-3, which possesses sequence features of the class II AUUUA-containing AREs. It has two overlapping UUAUUUAUU nonamers and six copies of the AUUUA motif within a highly U-rich region. Substitution of the IL-3 ARE with the ARE from either the

c-*fos* or c-*myc* 3′ UTR cannot restore the rapid degradation observed for the normal IL-3 ARE. Since the c-*fos* and c-*myc* AREs are considered class I AUUUA-containing AREs whereas the IL-3 ARE is considered class II, these findings suggest that there are differences in the regulation of the destabilizing

TABLE 1. Functional properties of three classes of ARE

ARE	Example	Decay kinetics	Mechanism of deadenylation reaction	Sensitivity to actinomycin D	Coupling to on-going translation by ribosomes	UUAUUUA(A/U)(A/U) motif as a functional requirement
AUUUA containing						
Class I	c-fos	Biphasic decay, synchronous poly(A) shortening	Distributive nucleolytic action; precedes decay of the RNA body	Sensitive	Not a stringent requirement	No
Class II	GM-CSF	Biphasic decay, asynchronous poly(A) shortening	Processive nucleolytic action; precedes decay of the RNA body	Sensitive	Not a stringent requirement	May need at least two overlapping copies
Non-AUUUA	c-jun	Biphasic decay, synchronous poly(A) shortening	Distributive nucleolytic action; precedes decay of the RNA body	Not sensitive	Not a stringent requirement	No

function between the two classes of AUUUA-containing ARE in IL-3-dependent mast cells. Thus, their data support the idea that different AREs may display cell state, cell type, or cell cycle-dependent destabilizing function. It will be interesting to determine whether the GM-CSF ARE, which is proposed to belong to the same class as the IL-3 ARE, can substitute for the IL-3 ARE in mast cells.

By use of synthetic AU-rich sequences, two groups reported that the key sequence motif necessary for directing rapid mRNA decay by AREs is a nonamer, UUAUUUA(U/A)(U/A) (13, 21). However, it should be noted that in the study by Zubiaga et al. (21), a 53-nt AU-rich (60% A+U residues) spacer that was thought to be neutral was inserted between the stop codon and the synthetic AU-rich sequences being tested. Given our observation that the c-jun ARE domain II (48 nt with 58% A+U residues) alone has no destabilizing ability but can greatly enhance the domain III destabilizing function when present upstream of it, the destabilizing effect seen for the combination of the 53-nt AU-rich spacer sequence plus a copy of the nonamer described in the study by Zubiaga et al. (21) could be a synergistic effect resulting from the combination of the two sequences rather than the nonamer alone. Our finding that neither the AUUUA nor the UUAUUUA(U/A)(U/A) motif is present in the c-jun ARE argues strongly that neither of these sequences is a key feature of all AREs. We propose that the nonamer may be required to specify the destabilizing function of class II AUUUA-containing AREs, which have at least two overlapping copies of this nonamer. Since mutagenesis experiments that specifically inactivate the nonamers in class II AUUUA-containing AREs have not been performed, the functional role of these nonamers in determining the destabilizing function of class II AREs remains to be confirmed.

Apart from the absence of the AUUUA or UUAUUUA(U/A)(U/A) motif, the other striking difference between the c-jun ARE and the two classes of AUUUA-containing AREs is the ability of the c-jun ARE to function in the presence of the transcription inhibitors actinomycin D and DRB. This finding further substantiates our hypothesis that the c-jun non-AUUUA ARE represents a new class of ARE. While the molecular basis underlying the differential stabilization effect of transcription inhibitors on a subset of AREs is not yet known, our preliminary experiments may shed some light on the mechanism. We have found a correlation between the sensitivity of an ARE to the actinomycin D retardation effect and its affinity for an actinomycin D-inducible ARE-binding factor detectable in in vitro experiments. For example, the c-jun ARE has a lower affinity for an actinomycin D-inducible RNA-binding factor than do the c-fos and GM-CSF AREs (unpublished observa-

tion), and it is also the least sensitive to actinomycin D and is insensitive to the DRB-induced decay retardation effect. It is possible that actinomycin D treatment of NIH 3T3 cells leads to an increase in this particular ARE-binding protein beyond a critical threshold in the cytoplasm. This, in turn, may result in a favorable shift in the binding of this factor to the high-affinity AREs, such as the c-fos and GM-CSF AREs. However, for the low-affinity substrates, such as the c-jun ARE, the cytoplasmic concentration of this factor is still below the level required to display the retardation effect (5). An implication of this hypothesis is that a redistribution to the cytoplasm of the actinomycin D-inducible factor or alteration of its affinity to AREs could be invoked by, e.g., signal transduction pathways during cell growth and differentiation as a way of achieving differential regulation of different ARE-containing mRNAs in a cell-state- or cell-type-specific manner.

Four separate studies have reported that the GM-CSF ARE requires that the mRNAs bearing it be translated for the ARE to exert its destabilizing function (1, 8, 15, 20). In addition, one of these studies also reported that the c-fos ARE appears to have a requirement for translation coupling for its destabilizing function (20). On the other hand, Koeller et al. (11) and Chen et al. (5) have shown that the c-fos ARE is able to exert its full destabilizing function when translation initiation of the mRNA carrying the ARE is blocked. Moreover, we have further shown that the GM-CSF ARE can also exhibit a translation-independent destabilizing function (5). Our conclusion is supported by polysome profile studies showing that upon hairpin blockage of translation initiation, more than 90% of the BBB+ARE mRNA cosediments with nontranslating 40 or 60S ribosomal subunits (5). Taken together with the finding from this study that the destabilizing function of c-jun ARE can also be uncoupled from ongoing translation by ribosomes, these data provide evidence to challenge any model proposing tight coupling between translation and ARE-directed mRNA decay. One possibility that reconciles the apparent discrepancy concerning the requirement of translational coupling for the GM-CSF and c-fos AREs is that in different cell types or stages of the cell cycle, AREs may exhibit a differential requirement for translation to act as a destabilizing element. For example, our studies show that during the G_0-to-G_1 transition in NIH 3T3 cells induced by serum stimulation of quiescent cells, all three classes of AREs display translation-independent destabilizing function. Under this condition, an alternative pathway that is independent of the translational status of the mRNA carrying the ARE may be operative. While elucidating the basis for these discrepant results awaits further experiments, it is clear that the destabilizing function of AREs is not tightly coupled to

ongoing translation by ribosomes. It will be important to further investigate to what extent and by what mechanisms the destabilizing function of each class of ARE is differentially regulated, such as in terminally differentiated cells, in mitotically synchronous cells, or in quiescent cells.

In conclusion, we have described several structural and sequence features, as well as functional properties (Table 1), which demonstrate the presence of distinct classes of ARE. We propose that each individual ARE may represent its own unique combination of modular sequences whose interactions determine the final destabilizing function of the ARE in terms of its decay kinetics, its sensitivity to actinomycin D, its dependency on translation coupling, and/or its cell state specificity. The difference in these characteristics may be more subtle among members of the same class than among different classes, and some domains appear functionally overlapping or redundant. We suspect that these modules are unlikely to display any high degree of sequence specificity. It will be challenging to identify and further characterize the key features of a group of functionally related domains that lead to their redundancy. The classification and the criteria we have described should prove useful as an experimental basis for further delineation of the mechanisms of ARE-directed mRNA degradation and their regulation.

ACKNOWLEDGMENTS

REFERENCES

1. **Aharon, T., and R. J. Schneider.** 1993. Selective destabilization of short-lived mRNAs with the granulocyte-macrophage colony-stimulating factor AU-rich noncoding region is mediated by a cotranslational mechanism. Mol. Cell. Biol. **13:**1971–1980.
2. **Akashi, M., G. Shaw, M. Hachiya, E. Elstner, G. Suzuki, and P. Koeffler.** 1994. Number and location of AUUUA motifs: Role in regulating transiently expressed RNAs. Blood **83:**3182–3187.
3. **Caput, D., B. Beutler, K. Hartog, R. Thayer, S. Brown-Shimer, and A. Cerami.** 1986. Identification of a common nucleotide sequence in the 3′-untranslated regions of mRNA molecules specifying inflammatory mediators. Proc. Natl. Acad. Sci. USA **83:**1670–1674.
4. **Chen, C.-Y. A., T.-M. Chen, and A.-B. Shyu.** 1994. Interplay of two functionally and structurally distinct domains of the c-*fos* AU-rich element specifies its mRNA-destabilizing function. Mol. Cell. Biol. **14:**416–426.
5. **Chen, C.-Y. A., N. Xu, and A.-B. Shyu.** 1995. mRNA decay mediated by two distinct AU-rich elements from c-*fos* and granulocyte-macrophage colony-stimulating factor transcripts: different deadenylation kinetics and uncoupling from translation. Mol. Cell. Biol. **15:**5777–5788.
6. **Chen, C.-Y. A., and A.-B. Shyu.** 1995. AU-rich elements: characterization and importance in mRNA degradation. Trends Biochem. Sci. **20:**465–470.
7. **Chen, C.-Y. A., and A.-B. Shyu.** 1994. Selective degradation of early-response-gene mRNAs: functional analyses of sequence features of the AU-rich elements. Mol. Cell. Biol. **14:**8471–8482.
8. **Curatola, A. M., M. S. Nadal, and R. J. Schneider.** 1995. Rapid degradation of AU-rich element (ARE) mRNAs is activated by ribosome transit and blocked by secondary structure at any position 5′ to the ARE. Mol. Cell. Biol. **15:**6331–6340.
9. **Higuchi, R.** 1990. Recombinant PCR, p. 177–183. *In* M. A. Innis, D. H. Gelfand, J. J. Sninsky, and T. J. White (ed.), PCR protocols: a guide to methods and applications. Academic Press, Inc., San Diego, Calif.
10. **Hirsch, H. H., P. K. Asha, V. Backenstoss, and C. Moroni.** 1995. Interleukin-3 mRNA stabilization by a trans-acting mechanism in autocrine tumors lacking interleukin-3 gene rearrangements. J. Biol. Chem. **270:**20629–20635.
11. **Koeller, D. M., J. A. Horowitz, J. L. Casey, R. D. Klausner, and J. B. Harford.** 1991. Translation and the stability of mRNAs encoding the transferrin receptor and c-*fos*. Proc. Natl. Acad. Sci. USA **88:**7778–7782.
12. **Kozak, M.** 1989. Circumstances and mechanisms of inhibition of translation by secondary structure in eucaryotic mRNAs. Mol. Cell. Biol. **9:**5134–5142.
13. **Lagnado, C. A., C. Y. Brown, and G. J. Goodall.** 1994. AUUUA is not sufficient to promote poly(A) shortening and degradation of an mRNA: the functional sequence within AU-rich elements may be UUAUUUA(U/A)(U/A). Mol. Cell. Biol. **14:**7984–7995.
14. **Ross, J.** 1995. mRNA stability in mammalian cells. Microbiol. Rev. **59:**16–95.
15. **Savant-Bhonsale, S., and D. W. Cleveland.** 1992. Evidence for instability of mRNAs containing AUUUA motifs mediated through translation-dependent assembly of a >20S degradation complex. Genes Dev. **6:**1927–1939.
16. **Shaw, G., and R. Kamen.** 1986. A conserved AU sequence from the 3′ untranslated region of GM-CSF mRNA mediates selective mRNA degradation. Cell **46:**659–667.
17. **Shyu, A.-B., J. G. Belasco, and M. E. Greenberg.** 1991. Two distinct destabilizing elements in the c-*fos* message trigger deadenylation as a first step in rapid mRNA decay. Genes Dev. **5:**221–231.
18. **Shyu, A.-B., M. E. Greenberg, and J. G. Belasco.** 1989. The c-*fos* transcript is targeted for rapid decay by two distinct mRNA degradation pathways. Genes Dev. **3:**60–72.
19. **Stoecklin, G., S. Hahn, and C. Moroni.** 1994. Functional hierarchy of AUUUA motifs in mediating rapid interleukin-3 mRNA decay. J. Biol. Chem. **269:**28591–28597.
20. **Winstall, E., M. Gamache, and V. Raymond.** 1995. Rapid mRNA degradation mediated by the c-*fos* 3′ AU-rich element and that mediated by the granulocyte-macrophage colony-stimulating factor 3′ AU-rich element occur through similar polysome-associated mechanisms. Mol. Cell. Biol. **15:**3796–3804.
21. **Zubiaga, A. M., J. G. Belasco, and M. E. Greenberg.** 1995. The nonamer UUAUUUAUU is the key AU-rich sequence motif that mediates mRNA degradation. Mol. Cell. Biol. **15:**2219–2230.